J. O. Dimmock, Solid State Commun. 8, 2021 (1970).
[11]K. Nassau and J. W. Shiever, J. Crystal Growth (to be published).
[12]J. J. Hopfield, in *Proceedings of the International Conference on the Physics of Semiconductors, Exeter*, 1962, edited by A. C. Strickland (Bartholomew Press, Dorking, England, 1962), p. 75.
[13]C. H. Henry and J. J. Hopfield (unpublished).
[14]B. Segall and G. D. Mahan, Phys. Rev. 171, 935 (1968).
[15]D. C. Reynolds, C. W. Litton, and T. C. Collins, Phys. Rev. 156, 881 (1967).
[16]C. H. Henry, K. Nassau, and J. W. Shiever, Phys. Rev. B 4, 2453 (1971).
[17]D. Berlincourt, J. Joffe, and L. R. Shiozowa, Phys. Rev. 129, 1009 (1963).

PHYSICAL REVIEW B VOLUME 5, NUMBER 2 15 JANUARY 1972

Excitation Spectra and Piezospectroscopic Effects of Magnesium Donors in Silicon*

L. T. Ho and A. K. Ramdas
Department of Physics, Purdue University, Lafayette, Indiana 47907
(Received 23 August 1971)

Excitation spectra of magnesium impurities diffused into undoped silicon as well as into silicon doped with group-III acceptors have been measured. In the former, magnesium is a heliumlike neutral donor (Mg^0) with excited states similar to those of group-V donors and close to the effective-mass positions; its ionization energy at liquid-helium temperature is 107.50 ± 0.04 meV. In specimens containing group-III impurities, with the magnesium partially compensated, excitation spectra are observed similar to those of group-V donors and that of Mg^0 except that the spacings between corresponding lines are approximately four times larger and the $1s(A_1) \rightarrow 2p_\pm$ transition is a closely spaced doublet, 0.2 meV apart. These features are consistent with a singly ionized heliumlike magnesium donor (Mg^+) and a small chemical splitting of the $2p_\pm$ state; the ionization energy is 256.47 ± 0.07 meV at liquid-helium temperature. The excitation spectrum of Mg^+ was also observed in specimens containing Mg^0 subjected to high-energy electron irradiation. Study of the piezospectroscopic effects shows that both Mg^0 and Mg^+ occupy a T_d-symmetry site with $1s(A_1)$ as the ground state. A value of 8.7 ± 0.2 eV has been deduced for the shear-deformation-potential constant Ξ_u of the $\langle 100 \rangle$ conduction-band minima of silicon.

I. INTRODUCTION

The behavior of group-V impurities as donors and of group-III impurities as acceptors in silicon and germanium represents one of the most extensively studied and best understood aspects of semiconductor physics. The substitutional nature of these impurities, the large dielectric constant of the host, and the effective mass of the bound carrier are the significant features of the model used to explain a variety of phenomena[1-3] associated with these donors and acceptors which are solid-state analogs of the hydrogen atom. It is also now well established that the group-II elements, zinc,[4,5] mercury,[6] and beryllium[7] in germanium and beryllium in silicon,[7] are solid-state analogs of the helium atom in that they are double acceptors; by compensation with group-V donors one can study these double acceptors in their singly ionized state which then are the analogs of singly ionized helium. The group-VI element sulfur when introduced into silicon[8-10] behaves like a heliumlike double donor; several sulfur donor centers have been discovered though the exact structures of these have not yet been established. For example, the electron paramagnetic resonance (EPR) measurements by Ludwig[9] showed that the sulfur centers designated as D centers by Krag *et al.*[8] are isolated S^+ at T_d sites, but he could not determine if they occupied the substitutional or the interstitial sites with that symmetry. The group-I impurity copper in germanium,[11] is another element which has been studied to some extent. The acceptor states associated with this impurity are consistent with its being substitutional.

Of the impurities which are interstitial rather than substitutional, the best-known example is that of lithium in silicon and germanium.[12,13] Transition-metal ions in silicon and germanium, both as interstitial and substitutional impurities, have been studied by Woodbury and Ludwig[14] who investigated their EPR spectra. Interstitial aluminum has been reported in electron-irradiated aluminum-doped silicon where interstitial silicon and substitutional aluminum are believed to exchange their roles[15]; it has been shown that these interstitial aluminum impurities are then donors. Recently,[16,17] the group-II element magnesium, when diffused into silicon, has been shown to behave like a double donor rather than a double acceptor. This behavior can be understood only if magnesium is interstitial rather than substitutional. Singly ionized magnesium donors can be produced by diffusing magnesium into

silicon containing acceptors[17] like boron or aluminum or by electron irradiation as well as by thermally ionizing neutral magnesium.[16] The purpose of the present paper is to report and discuss the results of a detailed study of the Lyman spectra associated with both neutral and singly ionized magnesium donors in silicon including their piezospectroscopic effects.

II. EXPERIMENTAL PROCEDURE

Magnesium was diffused into silicon in the following manner. Pure magnesium[18] was deposited by evaporation on the surfaces of the optical sample. The optical sample was sandwiched between two other specimens, all three having magnesium on the surfaces in contact, and heated at ~1200 °C for ~1 h in a helium atomosphere; the sample and the "covers" weld together and thus the magnesium does not escape into the ambient. After the heat treatment, the sample, together with the covers, was quenched in liquid nitrogen. The covers were then ground off. By following this procedure an undoped floating-zone silicon, initially p type and of resistivity ~1700 Ω cm, was converted to a low-resistivity n-type specimen with a room-temperature carrier concentration $\sim 2\times 10^{15}$ cm^{-3}. These specimens were adequate for observing the excitation spectra of neutral magnesium (Mg^0) at low temperatures. In order to study singly ionized magnesium (Mg^+) donors, low-resistivity ~10-Ω-cm boron-doped or aluminum-doped floating-zone silicon was used instead of pure silicon. From experience it was found that diffusion times of ~10 h were required to produce sufficient concentration of Mg^+ for the present studies. The samples were too inhomogeneous to give reliable Hall measurements. The boron concentration in most of the specimens used was $\sim 1.5\times 10^{15}$ cm^{-3} and such specimens showed only Mg^+ spectrum and no trace of Mg^0 spectrum; an upper limit of 10^{15} cm^{-3} of Mg^+ is thus estimated. It was also found that Mg^+ could be produced in specimens containing initially Mg^0 only, by subjecting them to an irradiation with high-energy electrons. In this case magnesium-doped silicon was irradiated with 1-MeV electrons from a Van de Graaff accelerator. Specimens subjected to the same heat treatment and quench failed to show the spectra if no magnesium was deposited on them initially; this check was made to satisfy ourselves that we are indeed dealing with magnesium centers, Mg^0 or Mg^+ as the case may be.

The samples used in these experiments were oriented for appropriate crystallographic orientations either by x rays or by the optical method of Hancock and Edelman.[19] An optical cryostat[20] was used for low-temperature measurements; sample temperatures ~12°K are estimated in our liquid-helium measurements. Uniaxial compression was applied to the specimens for piezospectroscopic measurements using the differential-thermal-compression technique.[21] In order to determine the shear-deformation-potential constant Ξ_u, a calibrated stress was employed in some of the piezospectroscopic measurements; this was accomplished using a quantitative-stress optical cryostat[22] which is an adaptation of the glass cryostat described in Ref. 20.

A double-pass Perkin-Elmer spectrometer, model 112G, equipped with Bausch-and-Lomb plane-reflection gratings and appropriate filtering systems, was used for the measurements. Typical resolution in our measurements is ~0.5 cm^{-1}. The radiation was polarized for piezospectroscopic measurements by passing it through a Perkin-Elmer wire-grid polarizer with silver-bromide substrate. A Reeder[23] thermocouple with a cesium-iodide window was used as the detector.

III. EXPERIMENTAL RESULTS AND DISCUSSION: Mg^0

A. Zero Stress

The excitation spectrum for neutral magnesium donors in silicon measured with liquid helium as coolant is shown in Fig. 1. The energies of the excitation lines are given in Table I. The excitation spectrum for phosphorus[24] donors in silicon drawn on the same energy scale as that of Fig. 1 is shown in Fig. 2 for comparison. It is evident that the lines of the two spectra are strikingly similar in spacing and relative intensities. This can also be seen from Table II where the spacings for the two spectra are compared. The labeling of the excitation lines for magnesium donor is based on this similarity. The half-width for the excitation lines of Mg^0 is approximately twice as large as that of the phosphorus lines. The factors contributing to this feature have yet to be established. The broadening of the lines could also be the rea-

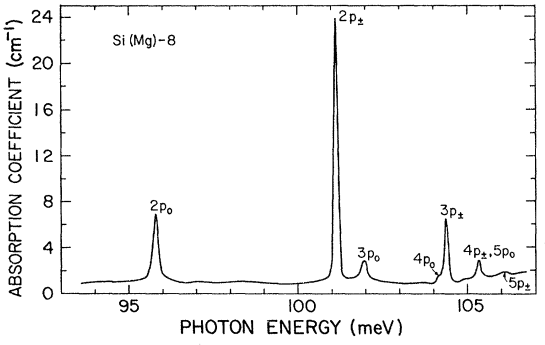

FIG. 1. Excitation spectrum of Mg^0 donors in silicon. Liquid helium was used as coolant. Carrier concentration, n(300 °K), estimated $\sim 1.2\times 10^{15}$ cm^{-3}.

TABLE I. Energies of excitation lines of Mg^0 donors in silicon (in meV).

Label	Assignment	Energy [a]
$2p_0$	$1s(A_1) \rightarrow 2p_0$	95.80
$2p_\pm$	$1s(A_1) \rightarrow 2p_\pm$	101.12
$3p_0$	$1s(A_1) \rightarrow 3p_0$	101.95
$4p_0$	$1s(A_1) \rightarrow 4p_0$	104.17
$3p_\pm$	$1s(A_1) \rightarrow 3p_\pm$	104.38
$4p_\pm, 5p_0$	$1s(A_1) \rightarrow 4p_\pm, 5p_0$	105.33
$5p_\pm$	$1s(A_1) \rightarrow 5p_\pm$	106.05
E_I [b]		107.50 ± 0.04

[a]The experimental error is ± 0.015 meV. These values are in good agreement with those reported by Franks and Robertson (see Ref. 16).

[b]The ionization energy E_I was deduced by adding Faulkner's theoretically determined binding energy of the $3p_\pm$ state (Ref. 26) to the experimental energy of the transition labeled $3p_\pm$.

son why the a and b lines in the phosphorus spectrum are not seen in the Mg^0 spectrum.

As an interstitial impurity the donor electrons of magnesium are expected to be the two $3s$ valence electrons thus constituting neutral heliumlike centers. When one of these electrons is excited, the screening of the nuclear charge by the remaining electron and the other core electrons should result in hydrogenic excited states. The higher the excited state the more accurate will be this description. Comparison of energy levels of atomic hydrogen and helium shows this to be the case.[25] We expect the screening to be particularly effective for the p-like final states in the $1s \rightarrow np$ transitions. The remarkable similarity of the spacings between the excited states of Mg^0 and those of the group-V donors is thus explained. In the same manner it is also clear why the spacings observed in the excitation spectrum of Mg^0 are strikingly close to those calculated[26] for group-V donors in the effective-mass theory.

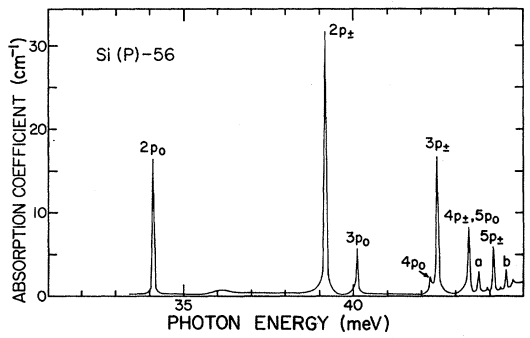

FIG. 2. Excitation spectrum of phosphorus donors in silicon. Liquid helium was used as coolant. $n(300\,°K) = 7.5 \times 10^{14}$ cm^{-3} (see Ref. 24).

As in the case of group-V donors, the positions of the excitation lines of Mg^0 will be determined by the location of the ground state which may lie below the effective-mass position due to the breakdown of the effective-mass theory in the vicinity of the impurity, giving the chemical splitting. The ground state is expected to be affected most seriously by this breakdown because of the large concentration of its wave function near the impurity core.[1] It is thus of interest to deduce the effective-mass ionization energy, which can perhaps be estimated by increasing the effective-mass ionization energy of group-V donors calculated by Faulkner[26] in the ratio of the first-ionization energy of the helium atom to that of the ionization energy of the hydrogen atom; this turns out to be $(31.27)(24.46)/(13.6) = 56.24$ meV. Here we have used the experimental values for the ionization energies of atomic helium and hydrogen, which, of course, are well known to be close to the calculated values [see Eyring, Walter, and Kimball (Ref. 27)]. The experimental ionization energy obtained by adding the calculated value[26] of the binding energy of the $3p_\pm$ state to the experimental energy of the transition labeled $3p_\pm$ in the Mg^0 spectrum is 107.50 meV; the justification for this procedure lies in the excellent agreement between the calculated and the experimental spacings of the excitation lines on the one hand and that between the spacings of the corresponding lines of phosphorus and magnesium donors on the other. Thus, it is evident that the ground state has suffered considerable chemical splitting. Presumably the sixfold degeneracy of the $1s$ state due to the multivalley nature of the conduction-band minima along $\langle 100 \rangle$ is lifted in the same manner as for group-V donors, and the ground state[27] is the totally symmetric linear combination $1s(A_1)$ with equal contribution of all the six $\langle 100 \rangle$ Bloch wave functions. The experimental proof for the singlet nature of the ground state will be forthcoming from the piezospectroscopic effects discussed in Sec. III B.

Recently Faulkner[26] has calculated in the effective-mass approximation the binding energies of energy

TABLE II. Spacings of donor excited states in silicon (meV).

States	Theory [a]	P [b]	Mg [b]
$2p_\pm - 2p_0$	5.11	5.06	5.32
$3p_0 - 2p_\pm$	0.92	0.93	0.83
$4p_0 - 2p_\pm$	3.07	3.09	3.05
$3p_\pm - 2p_\pm$	3.28	3.28	3.26
$4p_\pm - 2p_\pm$	4.21	4.21	4.21
$5p_0 - 2p_\pm$	4.17	4.21	4.21
$5p_\pm - 2p_\pm$	4.97	4.94	4.93

[a]Faulkner, see Ref. 26.

[b]The experimental error is ± 0.03 meV.

levels which are not expected to be observed in the Lyman spectrum, *viz.*, of $2s$, $3s$, $3d_0$, $4s$, $4d_0$, $4f_0$, . . . , etc. Though transitions from the $1s$ state to these levels are not allowed in the effective-mass approximation, they may become weakly allowed due to departures from it. Kleiner and Krag[28] have ascribed several weak lines to just such transitions. We have unsuccessfully searched for the corresponding transitions in the spectrum of Mg^0 in silicon. We can not rule out that the concentration of magnesium donors in the samples used was insufficient.

As mentioned already, a significant feature of the donor levels in silicon is the chemical splitting of the sixfold degenerate $1s$ ground state into singlet $1s(A_1)$, doublet $1s(E)$, and triplet $1s(T_2)$ levels, with $1s(E)$ and $1s(T_2)$ close to the effective-mass position and $1s(A_1)$ depressed considerably below it. In contrast to the case of shallower group-V donors,[29] it is not feasible to thermally populate the $1s(E)$ and $1s(T_2)$ for Mg^0 and observe excitation lines which originate from them. Attempts were made to observe the $1s(A_1) \rightarrow 1s(T_2)$ transition which is again allowed only to the extent of the breakdown of the effective-mass theory. Such transitions have been reported for bismuth donors in silicon,[30] and selenium and tellurium donors in aluminum antimonide.[31] However, we have been unsuccessful in observing the corresponding transitions in the spectral range from 41 to 95 meV. In the course of the above measurements we found several weak excitation lines at 87.18, 87.99, and 104.90 meV which occurred in only a few of the samples examined. They appear to be due to as yet unidentified centers.

Attention should be drawn here to the decrease in the intensity of the excitation spectrum when the same specimen is remeasured after a considerable lapse of time. Figure 3 shows a typical example of such a spectrum remeasured after 19 months. This may be a consequence of precipitation of magnesium. Time-dependent effects on donor excitation spectra have been noticed by Gilmer *et al.*[32] in the spectra associated with lithium-oxygen complexes and by Ludwig[9] in EPR studies of sulfur-doped silicon.

B. Piezospectroscopic Effect

The study of excitation spectra of donors and acceptors in semiconductors under uniaxial stress[3] —the piezospectroscopic effect—is very valuable in giving symmetry assignments to the energy levels and offers a direct means of determining deformation-potential constants. The relevent details applicable to the case of donor states[3,29,33] of a multivalley semiconductor are given below. The conduction-band minima of a multivalley semiconductor are shifted with respect to one another under the application of a uniaxial stress. The deformation-potential theory as applied to this problem by Herring[34] gives the shift in energy of the jth minimum as

$$\Delta E^j = (\Xi_d \delta_{\alpha\beta} + \Xi_u K_\alpha^{(j)} K_\beta^{(j)}) u_{\alpha\beta} , \tag{1}$$

where $K_\alpha^{(j)}$ and $K_\beta^{(j)}$ are components of a unit vector pointing from the center of the Brillouin zone towards the position in $\vec{k}$ space of the jth minimum. The subindex α or β designates a component along one of the cubic axes of the crystal, $u_{\alpha\beta}$ are the components of the strain tensor, and $\delta_{\alpha\beta}$ is the Kronecker-δ symbol. The symbols Ξ_d and Ξ_u are the dilatational- and shear-deformation-potential constants, respectively. In Eq. (1) a summation over α and β is implied. If it is assumed that both the dielectric constant and the effective masses characterizing the conduction-band minima are unaltered by strains used in the experiments, then, for a given valley, the energy-level scheme of a donor given in the effective-mass approximation will be unaffected by the stress. However, the energy-level schemes bearing different valley labels will be shifted relative to one another by the amounts given by Eq. (1). This will be true for all states well described by the effective-mass theory, for example, the p states.

Under a compressive force $\vec{F}$, the valleys $j = 1$, 2, 3, 4, 5, and 6 along [100], [$\bar{1}$00], [010], [0$\bar{1}$0], [001], and [00$\bar{1}$], respectively, have energy shifts ΔE^j given by

$$\vec{F} \parallel [100], \begin{cases} \Delta E^{1,2} = [\Xi_d(s_{11} + 2s_{12}) + \Xi_u s_{11}]T , & \text{(2a)} \\ \Delta E^{3-6} = [\Xi_d(s_{11} + 2s_{12}) + \Xi_u s_{12}]T ; & \text{(2b)} \end{cases}$$

$$\vec{F} \parallel [110], \begin{cases} \Delta E^{1-4} = \tfrac{1}{2}[2\Xi_d(s_{11} + 2s_{12}) + \Xi_u(s_{11} + s_{12})]T , & \text{(2c)} \\ \Delta E^{5,6} = [\Xi_d(s_{11} + 2s_{12}) + \Xi_u s_{12}]T ; & \text{(2d)} \end{cases}$$

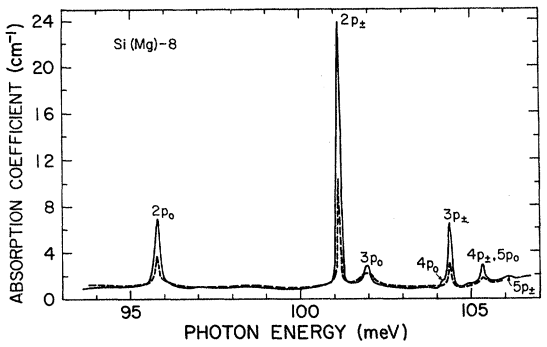

FIG. 3. Time-dependent effect on the excitation spectrum of Mg^0 donors in silicon. The dashed curve shows the decrease of intensity for the same sample remeasured after 19 months. Liquid helium was used as coolant in both measurements.

$\vec{F}\|[111]$, $\Delta E^{1-6} = \frac{1}{3}[3\Xi_d(s_{11}+2s_{12}) + \Xi_u(s_{11}+2s_{12})]T$, (2e)

where T is the applied force per unit area, and is defined to be positive for tension and negative for compression; the s_{ij}'s are the elastic compliance coefficients. It is thus clear that with $\vec{F}\|\langle 111\rangle$ there will be no splittings for the effective-mass donor states whereas for $\vec{F}\|\langle 100\rangle$ and $\vec{F}\|\langle 110\rangle$, a given donor level will split into two components whose shifts with respect to the center of gravity (c.g.) are given by

$$\vec{F}\|[100],\begin{cases}\Delta E^{1,2} - \Delta E_{\text{c.g.}} = \frac{2}{3}\Xi_u(s_{11}-s_{12})T\,, & \text{(3a)}\\ \Delta E^{3-6} - \Delta E_{\text{c.g.}} = -\frac{1}{3}\Xi_u(s_{11}-s_{12})T; & \text{(3b)}\end{cases}$$

$$\vec{F}\|[110],\begin{cases}\Delta E^{1-4} - \Delta E_{\text{c.g.}} = \frac{1}{6}\Xi_u(s_{11}-s_{12})T\,, & \text{(3c)}\\ \Delta E^{5,6} - \Delta E_{\text{c.g.}} = -\frac{1}{3}\Xi_u(s_{11}-s_{12})T. & \text{(3d)}\end{cases}$$

Wilson and Feher[35] have calculated the energies of the ground states $1s(A_1)$, $1s(E)$, and $1s(T_2)$ as a function of stress; the results are shown for $\vec{F}\|[100]$ in Fig. 4. The stress effect on a typical excited p state, the $2p_\pm$ state, is also shown in this figure for comparison. The labels on the stress-induced sublevels denote the irreducible representations of the new site symmetry to which they belong. As shown in the figure the shift of the singlet $1s(A_1)$ state shows a nonlinear dependence on stress. Both $1s(E)$ and $1s(T_2)$ states split into two components; one component of $1s(E)$ shifts linearly and the other nonlinearly with stress whereas both components of $1s(T_2)$ show a linear dependence on stress identical to that of the p states. It can be shown[12,29] that the transitions which have $1s(A_1)$ as their ground state should, under stress, exhibit two components, one on either side of the zero-stress position, while transitions from $1s$ (T_2) and $1s(E)$ exhibit one and three components, respectively.

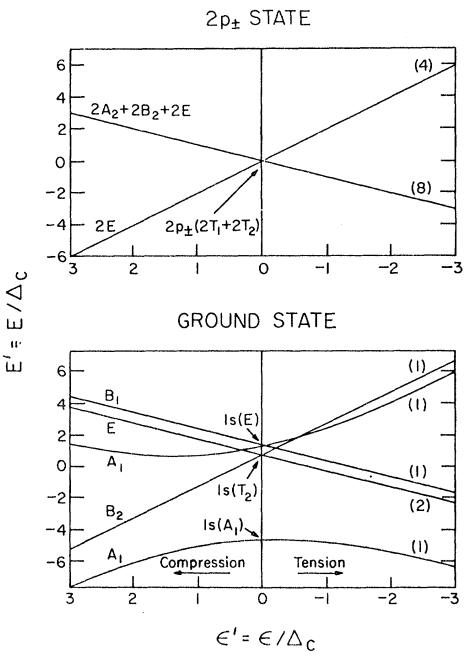

FIG. 4. Splitting of the $1s$ ground states and the $2p_\pm$ state of donors in silicon under strain for compressive force $\vec{F}$ along $\langle 100\rangle$. $E' = E/\Delta_c$ and $\epsilon' = \epsilon/\Delta_c$, where E is the energy of a given state. $\Delta_c = \frac{1}{6}$ [the spacing between $1s(A_1)$ and $1s(E)$], and 3ϵ is the energy difference between the $\langle 100\rangle$ conduction-band minima. The numbers in parentheses indicate the degeneracies of the various states while the letters denote the relevant irreducible representations of D_{2d}, the site symmetry of the donor for this direction of stress.

It should be noted that, though the $1s(A_1) \rightarrow np$ excitation lines will not split under $\vec{F}\|\langle 111\rangle$, they may show shifts due to those of the $1s(A_1)$ ground state. The separation between the two components observed for $\vec{F}\|\langle 100\rangle$ or $\langle 110\rangle$ is the same for all the lines. If the $1s(A_1)$ level undergoes only very small shifts, then the energy difference between the low-energy component and the zero-stress position will be twice that between the high-energy component and the zero-stress position for $\vec{F}\|\langle 100\rangle$ and *vice versa* for $\vec{F}\|\langle 110\rangle$.

Another important feature of the uniaxial stress effect is the pronounced polarization exhibited by the stress-induced components of the excitation lines. The selection rules for electric-dipole transitions are shown in Figs. 5 and 6 for compression along [100] and [110], respectively, for the $1S(A_1) \rightarrow np_0$, and $np_\pm$ transitions. These can be deduced[3,33] either by group theory or by an intensity calculation using linear combinations of wave functions appropriate for the new site symmetry of the impurity. The new site symmetry is deduced by enquiring which symmetry operations of the unperturbed crystal continue to be valid under stress. Thus, the T_d site symmetry is transformed into the tetragonal D_{2d} under $\vec{F}\|[100]$ and into the orthorhombic C_{2v} under $\vec{F}\|[110]$. From Fig. 5 for $\vec{F}\|[100]$, it can be seen that for $\vec{E}\|\vec{F}$, only transitions $1s(A_1) \rightarrow np_0(-)$ and $np_\pm(+)$ are allowed, while for $\vec{E}\perp\vec{F}$, transitions $1s(A_1) \rightarrow np_0(+)$, $np_\pm(-)$, and $np_\pm(+)$ are allowed. For $\vec{F}\|[110]$ in Fig. 6, the selection rules also depend on the direction of the light-propagation vector, $\vec{q}$. For $\vec{E}\|\vec{F}$, $1s(A_1) \rightarrow np_0(-)$, $np_\pm(-)$, and $np_\pm(+)$ are allowed for all $\vec{q}$, and for $\vec{E}\perp\vec{F}$, $1s(A_1) \rightarrow np_0(-)$, $np_0(+)$, and $np_\pm(-)$ are allowed for $\vec{q}\|[1\bar{1}0]$, while $1s(A_1) \rightarrow np_0(-)$, $np_\pm(-)$, and $np_\pm(+)$ are allowed for $\vec{q}\|[001]$.

Let us now look at the experimental observations presented in Figs. 7–10 for uniaxial compression

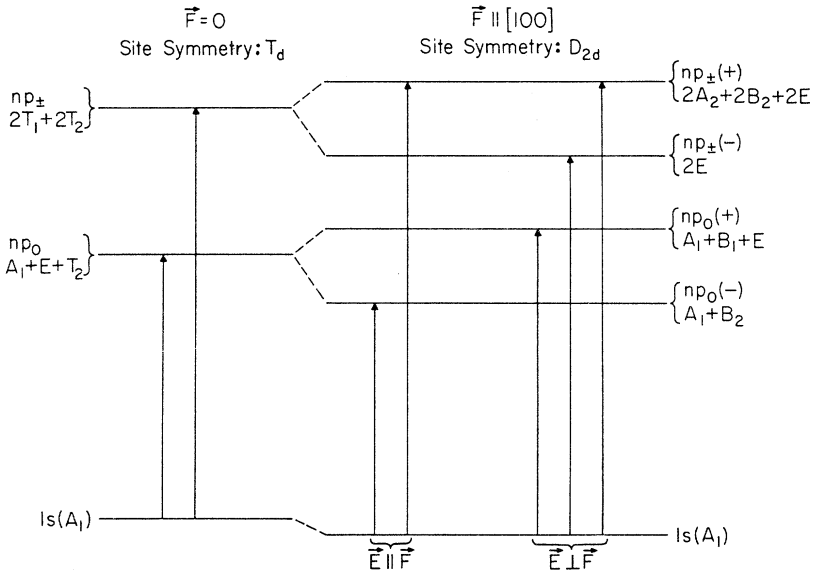

FIG. 5. Energy levels (not to scale) for $\vec{F}=0$ and $\vec{F} \parallel \langle 100 \rangle$. The arrows indicate the allowed transitions with $1s(A_1)$ as the ground state. The letters next to a level denote the irreducible representations of the appropriate site symmetry.

along [111], [100], [110], and [110], respectively, and for electric vector $\vec{E}$ either parallel or perpendicular to $\vec{F}$. In these figures the positions of the excitation lines for zero stress are also indicated.

In Fig. 7, for $\vec{F} \parallel [111]$, no splittings are observed. This is consistent with Eq. (2e) together with either the tetrahedral T_d or the tetragonal D_{2d}-symmetry site for the neutral magnesium donors, since any departure from these symmetries would have resulted in splittings due to the lifting of an orientational degeneracy associated with a noncubic environment.[36] For example, splittings precisely due to the lifting of such an orientational degeneracy have been reported by Krag *et al.* for certain species of sulfur donors in silicon.[8]

In the case of $\vec{F} \parallel [100]$ shown in Fig. 8, all the excitation lines split into two components, one on either side of the zero-stress position. We therefore conclude that all the observed transitions originate from $1s(A_1)$ as their ground state and that the site symmetry is T_d, not D_{2d}. For small stresses, as predicted in Eqs. (3a) and (3b), the low-energy components have an energy shift from the zero-stress position twice as large as that of the high-energy components. Furthermore, the polariza-

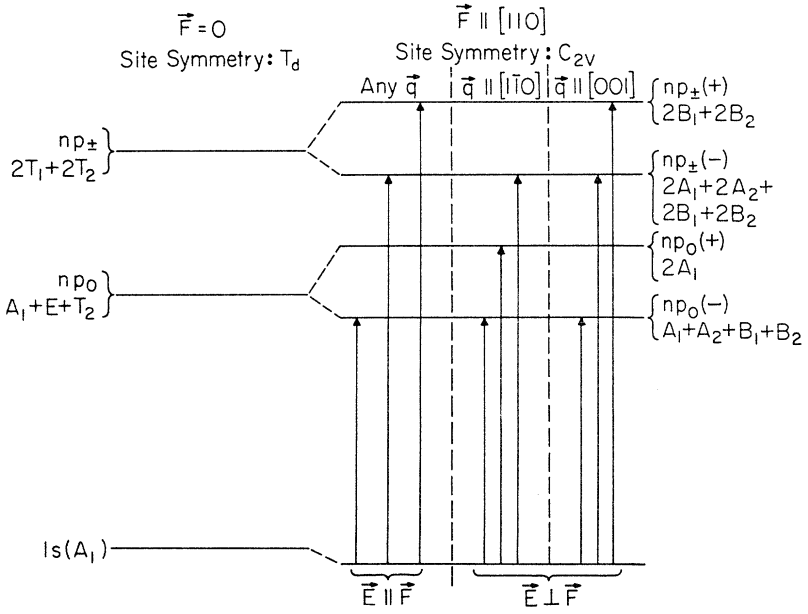

FIG. 6. Energy levels (not to scale) for $\vec{F}=0$ and $\vec{F} \parallel [110]$. The arrows indicate the allowed transitions with $1s(A_1)$ as the ground state and for the direction of light propagation $\vec{q}$ along [1$\bar{1}$0] and [001]. The letters next to a level denote the irreducible representations of the appropriate site symmetry. Note that a calculation (Ref. 33) of the intensity of the transition $1s(A_1) \rightarrow np_0(-)$, using effective-mass wave functions, shows it to be forbidden for $\vec{E} \perp \vec{F}$ and $\vec{q} \parallel [1\bar{1}0]$.

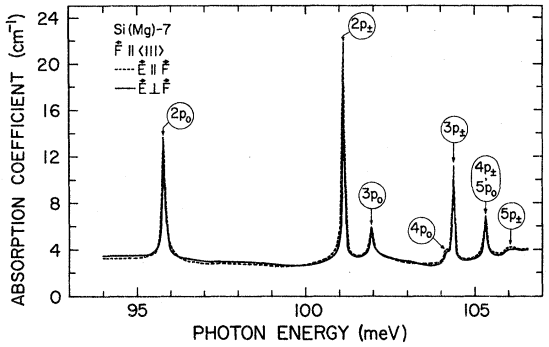

FIG. 7. Excitation spectrum of Mg^0 in silicon, with liquid helium as coolant and with $\vec{F} \parallel \langle 111 \rangle$. $n(300\,^\circ\mathrm{K}) = 2.7 \times 10^{15}\ \mathrm{cm}^{-3}$. The dashed curve is for $\vec{E} \parallel \vec{F}$ and the solid curve is for $\vec{E} \perp \vec{F}$. The arrows indicate the positions of the excitation lines for $\vec{F} = 0$.

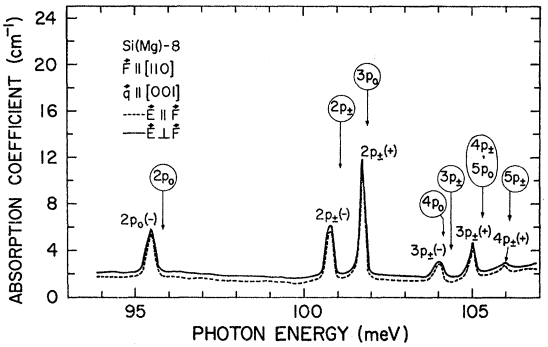

FIG. 9. Excitation spectrum of Mg^0 in silicon with liquid helium as coolant and with $\vec{F} \parallel [110]$ and $\vec{q} \parallel [001]$. $n(300\,^\circ\mathrm{K})$ was estimated to be $\sim 1.2 \times 10^{15}\ \mathrm{cm}^{-3}$. The dashed curve is for $\vec{E} \parallel \vec{F}$ and the solid curve is for $\vec{E} \perp \vec{F}$. The arrows indicate the positions of the excitation lines for $\vec{F} = 0$.

tion features completely agree with the predictions of Fig. 5, the high-energy component of the np_0 line appearing only for $\vec{E} \perp \vec{F}$ and the low-energy component only for $\vec{E} \parallel \vec{F}$, and both components of the $np_\pm$ line appearing for $\vec{E} \perp \vec{F}$ and only the high-energy components for $\vec{E} \parallel \vec{F}$.

In Figs. 9 and 10 are shown the results for $\vec{F} \parallel [110]$ with $\vec{q} \parallel [001]$ and $\vec{q} \parallel [1\bar{1}0]$, respectively. Both the splittings of the excitation lines and the polarization features agree with the selection rules given in Fig. 6 and Eqs. (3c) and (3d).

When a uniaxial stress is applied along an arbitrary direction, it can be shown from Eq. (1) that the six valleys will form three sets with each set having a different energy shift. As already mentioned, the excited p states will split into as many components as there are energetically different valleys. It is thus expected, for a stress along an arbitrary direction, each excitation line will split into three components.[37] In some of the measurements made, three components were indeed observed due to the misorientation of the ⟨110⟩ samples.

The shear-deformation-potential constant Ξ_u can be determined from the splittings of the excitation lines in a uniaxial stress measurement. A quantitative stress cell[22] was used for this purpose. Figure 11 shows a typical example of such measurements. For $\vec{F} \parallel [100]$, a given donor level, under stress T, splits into two components with their separation equal to $\Xi_u(s_{11} - s_{12})T$, as can be seen from Eq. (3). Figure 11 shows the energy spacing between the two components of $2p_\pm$ as a function of applied stress. From the slope we obtain for Ξ_u a value of 8.7 ± 0.2 eV.

The shift of the ground state $1s(A_1)$ under stress can also be determined from the above measurement. In Fig. 12, the positions of two experimentally observed components of the $1s(A_1) \rightarrow 2p_\pm$ tran-

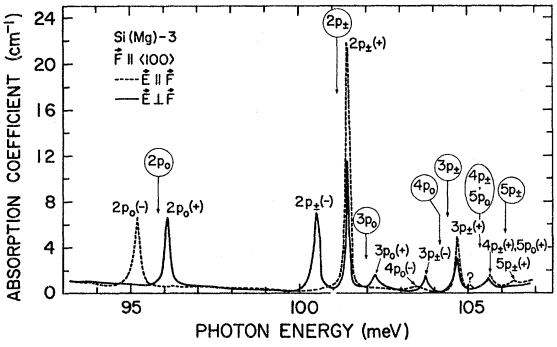

FIG. 8. Excitation spectrum of Mg^0 in silicon with liquid helium as coolant and with $\vec{F} \parallel \langle 100 \rangle$. $n(300\,^\circ\mathrm{K}) = 1.7 \times 10^{15}\ \mathrm{cm}^{-3}$. The dashed curve is for $\vec{E} \parallel \vec{F}$ and the solid curve is for $\vec{E} \perp \vec{F}$. The arrows indicate the positions of the excitation lines for $\vec{F} = 0$.

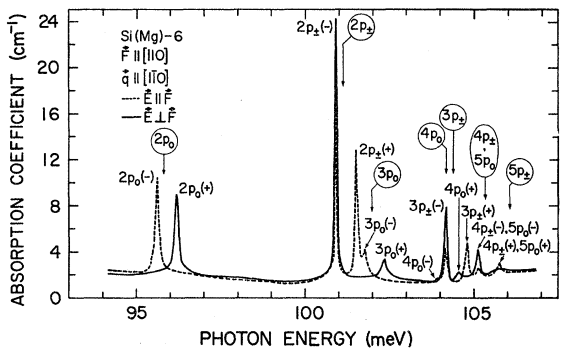

FIG. 10. Excitation spectrum of Mg^0 in silicon with liquid helium as coolant and with $\vec{F} \parallel [110]$ and $\vec{q} \parallel [1\bar{1}0]$. $n(300\,^\circ\mathrm{K}) = 2.1 \times 10^{15}\ \mathrm{cm}^{-3}$. The dashed curve is for $\vec{E} \parallel \vec{F}$ and the solid curve is for $\vec{E} \perp \vec{F}$. The arrows indicate the positions of the excitation lines for $\vec{F} = 0$.

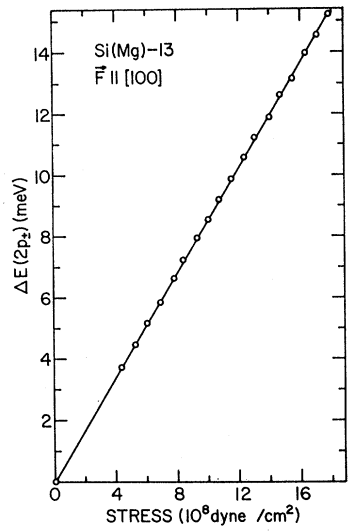

FIG. 11. The energy separation of the two stress induced components of the $2p_{\pm}$ line of Mg^0 in silicon as a function of stress. The compressive force $\vec{F}$ is along ⟨100⟩. The straight line represents a least squares fit; the experimental error is ±0.1 meV in ΔE and $\pm 0.2 \times 10^8$ dyn/cm^2 in stress.

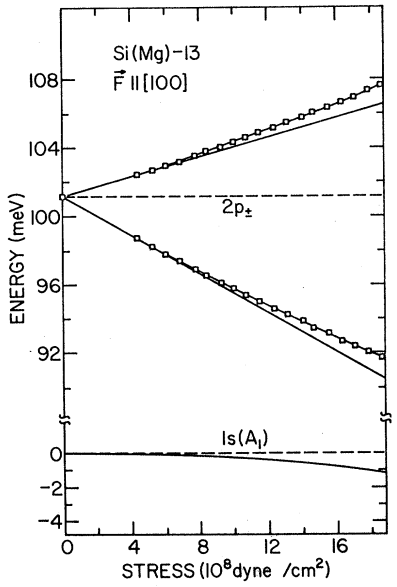

FIG. 12. Effect of uniaxial stress on the $2p_{\pm}$ and $1s(A_1)$ states of Mg^0 in silicon. The compressive force $\vec{F}$ is along ⟨100⟩. The positions indicated are those of the two observed components of the $1s(A_1) \rightarrow 2p_{\pm}$ transition as a function of stress. The experimental error in the position of each line is estimated to be ±0.05 meV and that in stress to be $\pm 0.2 \times 10^8$ dyn/cm^2. Their energy shifts from the zero-stress position in the ratio of 2:1 are shown by the two solid straight lines. From the actual observed energy positions, the shifts of $1s(A_1)$ are determined; the solid curve shows its shift as a function of stress.

sition are shown as a function of stress. Also shown, with solid lines, are their energy shifts from the zero-stress position as calculated from their spacings divided in the ratio 2:1. From the actual observed energy positions, the ground state shifts are thus deduced; the resulting shift of the $1s(A_1)$ ground state is also shown in the figure. Compared with shallow group-V donors, the ground-state shift of Mg^0 is found to be smaller as indeed it should be, for the deeper the ground state, the less it is influenced by stress, as can be seen from the calculations of Wilson and Feher.[35] For stresses less than 5×10^8 dyne/cm^2, the shift of $1s(A_1)$ can almost be neglected. The stress-dependent energy shift ΔE, of the $1s(A_1)$ ground state is given by

$$\Delta E = \Delta_c \left[3 + \tfrac{1}{2}x - \tfrac{3}{2}(x^2 + \tfrac{4}{3}x + 4)^{1/2} \right], \qquad (4)$$

where Δ_c is $\frac{1}{6}$ of the spacing between $1s(A_1)$ and $1s(E)$, and $x = \Xi_u(s_{11} - s_{12})T/3\Delta_c$. Knowing the energy shift of $1s(A_1)$ under a stress T, it is possible to solve for the spacing between $1s(A_1)$ and $1s(E)$, i.e., $6\Delta_c$. Using the experimentally determined value of 8.7 eV for Ξ_u, we obtain for $6\Delta_c$ a value of 55 ± 3 meV. Subtracting this from the ionization energy 107.50 meV, an experimental value of 52.5 ± 3 meV is obtained for the binding energy of the excited $1s(E)$ state; presumably the $1s(T_2)$ lies close to this if the separation between it and $1s(E)$ is small compared to $6\Delta_c$ as in the case of group-V donors. This appears to suggest that our earlier estimate for the effective-mass first-ionization energy, *viz.*, 56.24 meV, is reasonable for heliumlike donors in silicon. It also suggests that the $1s(E)$ and $1s(T_2)$ states are close to the effective-mass position while $1s(A_1)$ is depressed considerably below it due to chemical splitting.

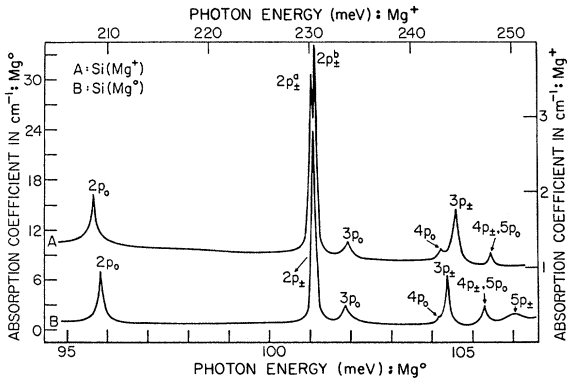

FIG. 13. Excitation spectra of Mg^0 and Mg^+ donors in silicon. Liquid helium was used as coolant. Mg^+ was produced by compensating Mg^0 with boron acceptors. Note that the energy scale for Mg^0 is four times larger than that for Mg^+.

TABLE III. Energies of excitation lines of Mg^+ donors in silicon (in meV).

Label	Assignment	Energy[a]
$2p_0$	$1s(A_1) \rightarrow 2p_0$	208.63 ± 0.015
$2p_\pm^a$	$1s(A_1) \rightarrow 2p_\pm^a$	230.22 ± 0.015
$2p_\pm^b$	$1s(A_1) \rightarrow 2p_\pm^b$	230.42 ± 0.015
$3p_0$	$1s(A_1) \rightarrow 3p_0$	233.87 ± 0.015
$4p_0$	$1s(A_1) \rightarrow 4p_0$	243.00 ± 0.045
$3p_\pm$	$1s(A_1) \rightarrow 3p_\pm$	243.99 ± 0.015
$4p_\pm$, $5p_0$	$1s(A_1) \rightarrow 4p_\pm$, $5p_0$	247.92 ± 0.015
E_I[b]		256.47 ± 0.07

[a]These values are larger by about 1 meV than those reported by Franks and Robertson (see Ref. 16). It should be noted, however, that the latter were obtained from a measurement at 135 °K. We have observed a shift to lower energies by ~ 0.3 meV in going from liquid-helium to liquid-nitrogen temperature. Such shifts taken together with larger uncertainties in positions at the higher temperature due to line broadening can account for the difference.

[b]The ionization energy E_I was deduced by adding four-times Faulkner's theoretically determined binding energy of the $3p_\pm$ state (Ref. 26) to the experimental energy of the transition labeled $3p_\pm$.

IV. EXPERIMENTAL RESULTS AND DISCUSSION: Mg^+

A. Zero Stress

The excitation spectrum for Mg^+ donors in silicon measured with liquid helium as coolant is shown in Fig. 13. The energies of the excitation lines are given in Table III. The excitation spectrum for Mg^0 donors in silicon is also shown in the same figure for comparison; note the energy scale for Mg^0 is four times larger than that for Mg^+ and the strongest line of Mg^0 spectrum, corresponding to $1s(A_1) \rightarrow 2p_\pm$, is brought into coincidence with the strongest line of Mg^+ spectrum. It is to be noted that the half-width for the excitation lines of Mg^+ is approximately four times as large as that of the Mg^0 lines. This might explain why the lines corresponding to the $5p_\pm$, a and b lines in the phosphorus spectrum in Fig. 2 are not observable in the Mg^+ spectrum.

While the interstitial Mg^0 is a solid-state analog of the helium atom as already mentioned, Mg^+ can be considered as the analog of singly ionized helium when one of its two 3s valence electrons is ionized. In this manner, then, the Lyman spectrum associated with Mg^+ donors is expected to be like those of group-V and Mg^0 donors in silicon except that the binding energy for each energy state is increased by a factor of 4 since now the effective nuclear charge is 2 instead of 1. This explains why in Fig. 13 the two spectra are strikingly similar in relative intensities and why the energy separations between the corresponding lines of Mg^+ are ~4 times the corresponding spacings of Mg^0. The labeling of the excitation lines for Mg^+ donors is based on this comparison.

Presented in Table IV is the comparison of energy spacings for excited states of Mg^+ and Mg^0 in silicon. The ratio of the corresponding spacings is approximately 4 as expected. It should be noted, however, that the ratio is not exactly 4 but slightly larger. This could be due to the penetration of the donor electron, the 3s valence electron, inside the inner electron shell.[38] Thus each energy state could be more tightly bound than the corresponding state neglecting this effect. Also, the lower energy state is expected to be affected more than the higher energy state. This should also apply to Mg^0; however, since there is another 3s electron which provides shielding, the donor electron may not penetrate the inner electron shell as much, thus resulting in a smaller effect. Besides this, the orbits of Mg^+ should be smaller than those for the other donors.

As in the case of Mg^0, it is of interest to estimate the effective-mass ionization energy for Mg^+. It is reasonable to assume this to be four times the effective-mass ionization energy of group-V donors calculated by Faulkner, i.e., 125.08 meV. The experimental ionization energy obtained by adding four times the theoretical value of the binding energy of the $3p_\pm$ state to the experimental energy of the transition labeled $3p_\pm$ is 256.47 meV. It is thus quite clear that the ground state has suffered a very large chemical splitting. As in the case for Mg^0, it turns out that for Mg^+ the singlet $1s(A_1)$ state is the ground state, the experimental proof for which is presented in Sec. IV B. As in the case of Mg^0, quantitative stress measurements can provide a determination of the chemical splitting; such measurements have not yet been made.

A noteworthy feature in the Mg^+ spectrum shown in Fig. 13 is the doublet nature of the $2p_\pm$ line, $2p_\pm^a$ and $2p_\pm^b$. At liquid-nitrogen temperature this feature is obscured due to broadening. At liquid-helium temperature this splitting was observed in the samples irrespective of the method used for compensation. It is tempting to ascribe this to the chemical splitting of the excited states. The irre-

TABLE IV. Comparison of energy spacings for excited states of Mg^0 and Mg^+ donors in silicon (in meV).

States	Mg^+	Mg^0	Ratio
$3p_\pm - 2p_0$	35.36 ± 0.03	8.58 ± 0.03	4.12 ± 0.02
$3p_\pm - 2p_\pm$	(a) 13.77 ± 0.03	3.26 ± 0.03	4.22 ± 0.05
	(b) 13.57 ± 0.03		4.16 ± 0.05
$3p_\pm - 3p_0$	10.12 ± 0.03	2.43 ± 0.03	4.17 ± 0.06
$3p_\pm - 4p_0$	0.99 ± 0.06	0.21 ± 0.03	4.78 ± 0.97
$4p_\pm$, $5p_0 - 3p_\pm$	3.93 ± 0.03	0.95 ± 0.03	4.14 ± 0.16

ducible representation for the $2p_\pm$ state is $2T_1+2T_2$ for a T_d-donor site symmetry. It could be that this state, due to chemical splitting, splits into two T_1+T_2 states, or even four states with two belonging to T_1 and the other two belonging to T_2. Since the transition from the $1s(A_1)$ ground state is allowed to an excited state belonging to T_2 and not to T_1, a doublet feature is thus expected in either case. Though the $2p_\pm$ state of Mg^+ donors is still expected to be effective-mass-like, compared with the corresponding state of group-V and Mg^0 donors, its binding energy is four times larger with a smaller Bohr radius and hence a larger chemical splitting. This perhaps explains why the doublet feature of the $2p_\pm$ state is not observed in the group-V and Mg^0 spectra. The $2p_0$ state lies even deeper than the $2p_\pm$ state; it should have thus suffered a larger chemical splitting. It should be noted, however, that the symmetry of the $2p_0$ state is given by the combination of irreducible representations A_1+E+T_2, and the transition from the $1s(A_1)$ ground state is allowed only to an excited state belonging to T_2. Thus no splitting would be observed for the $2p_0$ line, even if the final T_2 state had a chemical shift. As for the $3p_\pm$ and higher states, chemical splitting is presumably too small to be observed.

Attempts were again made to observe the $1s(A_1) \rightarrow 1s(T_2)$ transition for Mg^+, which is expected to be $\sim 256.47 - 125.08 = 131.39$ meV, if the excited $1s$ states are still close to the effective-mass position. No excitation lines, however, were observed in the spectral range from 107 to 135 meV. Similar attempts were also made to observe the even-parity levels like $2s$, $3s$, $3d_0$, ... etc., for Mg^+. An excitation line at 248.80 meV occurred only in some of the samples examined. It lies to the higher energy side of the $4p_\pm$, $5p_0$ line. Its intensity is somewhat larger than that of the $4p_\pm$, $5p_0$ line. Its position, however, does not agree with any of the calculated donor levels.[26] This line thus appears to be due to some as yet unidentified center. In one of the samples examined, three extra excitation lines were observed at 238.66, 239.60, and 241.26 meV, respectively. They fall near the region of $3s$ and $3d_0$. Again, since these lines are not reproducible in other samples, their origin is not certain.

As mentioned earlier, irradiation of magnesium-doped silicon with high-energy electrons was one of the methods of compensation used for producing Mg^+ donors. Extensive studies[15] have shown that a variety of donor as well as acceptor states associated with vacancies, interstitials, and their complexes are produced in silicon as a result of irradiation with high-energy electrons; with sufficient irradiation the Fermi level moves towards the middle of the energy gap. It is thus to be expected that compensation of Mg^0 could occur yielding Mg^+ donors. It is also possible[39,40] that the compensation occurs in the following manner: A vacancy moves close to the interstitial magnesium donor, or *vice versa* and is annihilated yielding substitutional magnesium. The latter should be a double acceptor which in turn can compensate the magnesium donors. This is an intriguing possibility which needs further study. In this context it should be particularly interesting to discover in irradiated specimens excitation spectra characteristic of acceptors in silicon.

The magnesium-doped silicon samples studied in the present work were irradiated with 1-MeV electrons at 10 °C. Magnesium donors were only partially compensated after irradiation; thus both Mg^0 and Mg^+ spectra can be observed in the same specimen. In most of the samples compensated with group-III acceptors, the control was not sufficient to produce partial compensation and hence Mg^0 and Mg^+ excitation spectra were not observed in the same specimen. A typical example is presented in Fig. 14 which shows the appearance of the Mg^+ spectrum and a decrease in that of Mg^0 as a result of electron irradiation. It is clear that the concentration of the Mg^0 donors is decreased while the excitation spectrum for Mg^+ appears only after the sample is bombarded.

B. Piezospectroscopic Effect

In Figs. 15–19 are presented the excitation spectra of Mg^+ donors in silicon for uniaxial compression along ⟨111⟩, ⟨100⟩, and ⟨110⟩, and for electric vector $\vec{E}$ either parallel or perpendicular to $\vec{F}$. In these figures the positions of the excitation lines for zero stress are also indicated.

The absence of splittings observed for the excitation lines in Fig. 15 with $\vec{F} \parallel \langle 111 \rangle$ is consistent with Eq. (2e) together with a site symmetry T_d or

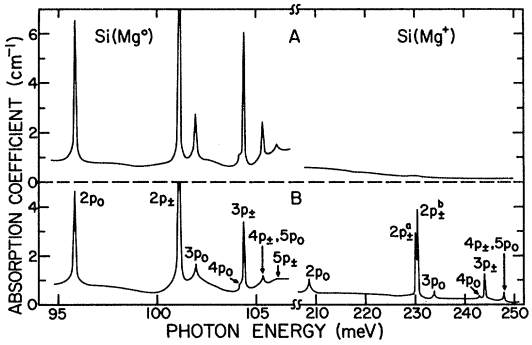

FIG. 14. Effect of 1-MeV electron irradiation on a magnesium-doped silicon sample. Excitation spectra of both Mg^0 and Mg^+ were measured using liquid helium as the coolant. *A* and *B* show the spectrum before and after the irradiation, respectively. The energy scale for Mg^0 is four times larger than that for Mg^+.

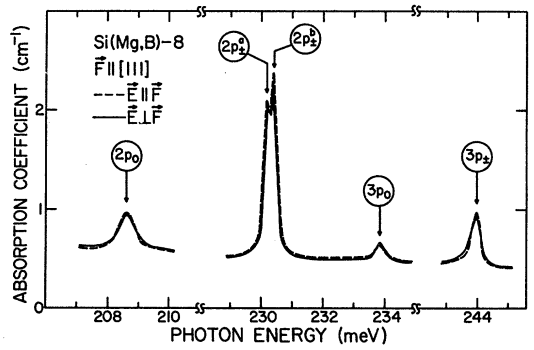

FIG. 15. Excitation spectrum of Mg^+ in silicon with liquid helium as coolant and with $\vec{F} \parallel \langle 111 \rangle$. Mg^+ was produced by compensating Mg^0 with boron acceptors. The dashed curve is for $\vec{E} \parallel \vec{F}$ and the solid curve is for $\vec{E} \perp \vec{F}$. The arrows indicate the positions of the excitation lines for $\vec{F} = 0$.

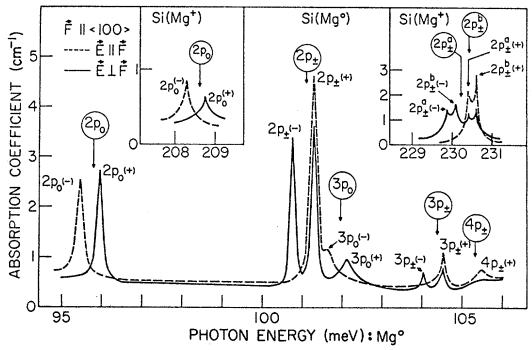

FIG. 17. Effect of a compressive force $\vec{F}$ along $\langle 100 \rangle$ on the excitation spectrum of Mg^0 in silicon. Liquid helium was used as coolant. The insets are for the $2p_0$, $2p^a_\pm$, and $2p^b_\pm$ lines of Mg^+ in the same specimen, partial compensation in it being achieved by electron irradiation. The dashed curve is for $\vec{E} \parallel \vec{F}$ and the solid curve is for $\vec{E} \perp \vec{F}$. The arrows indicate the positions of the excitation lines for $\vec{F} = 0$.

D_{2d}. In Fig. 16, for $\vec{F} \parallel \langle 100 \rangle$, all the excitation lines are observed to split into two components with one on either side of the zero-stress position. This strongly suggests that the interstitial singly ionized magnesium also occupies the T_d site with $1s(A_1)$ as the ground state. The polarization features also completely agree with Fig. 5, the high-energy component of the np_0 line appearing only for $\vec{E} \perp \vec{F}$, while the low-energy component, only for $\vec{E} \parallel \vec{F}$, and both the components of the $np_\pm$ line appearing for $\vec{E} \perp \vec{F}$ while only the high-energy component for $\vec{E} \parallel \vec{F}$. It should be noted here that shifts of the stress-induced components of the doublet $2p^a_\pm$ and $2p^b_\pm$ should be expected to include the effect of the chemical splittings; however, this difference appears to be too small to be observed in the present measurements. Also, the resolution in the measurement did not allow a clear separation of $2p^a_\pm(+)$ and $2p^a_\pm(-)$ from $2p^b_\pm(+)$ and $2p^b_\pm(-)$, respectively, for $\vec{E} \perp \vec{F}$. The spacing between the corresponding high- and low-energy components is, within experimental error, the same for all the lines.

In Fig. 17, results for a uniaxial compressive force $\vec{F}$ along $\langle 100 \rangle$ are presented for a specimen containing both Mg^0 and Mg^+ donors as a result of a partial compensation achieved by electron irradiation. The piezospectroscopic effect of the excitation spectrum of Mg^0 donors is identical to that given in Fig. 8. The insets in the figure show the splittings for the $2p_0$, $2p^a_\pm$, and $2p^b_\pm$ lines of Mg^+ donors during the same measurement. The results demonstrate that the corresponding lines of Mg^0 and Mg^+ show identical splittings and polarization

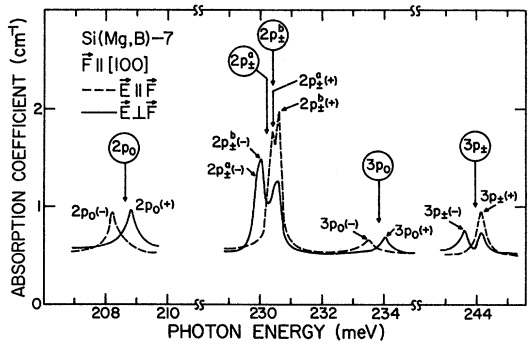

FIG. 16. Excitation spectrum of Mg^+ in silicon with liquid helium as coolant and with $\vec{F} \parallel \langle 100 \rangle$. Mg^+ was produced by compensating Mg^0 with boron acceptors. The dashed curve is for $\vec{E} \parallel \vec{F}$ and the solid curve is for $\vec{E} \perp \vec{F}$. The arrows indicate the positions of the excitation lines for $\vec{F} = 0$.

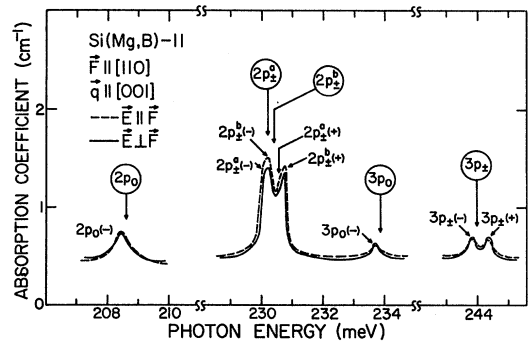

FIG. 18. Excitation spectrum of Mg^+ in silicon with liquid helium as coolant and with $\vec{F} \parallel [110]$ and $\vec{q} \parallel [001]$. Mg^+ was produced by compensating Mg^0 with boron acceptors. The dashed curve is for $\vec{E} \parallel \vec{F}$ and the solid curve is for $\vec{E} \perp \vec{F}$. The arrows indicate the positions of the excitation lines for $\vec{F} = 0$.

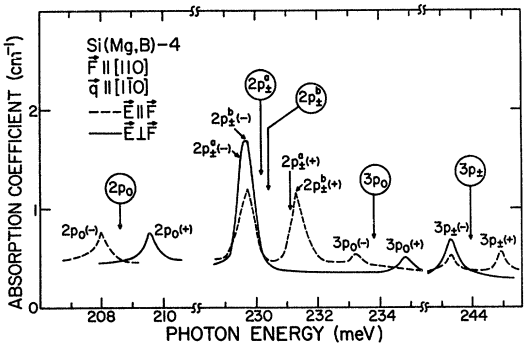

FIG. 19. Excitation spectrum of Mg^+ in silicon with liquid helium as coolant and with $\vec{F} \parallel [110]$ and $\vec{q} \parallel [1\bar{1}0]$. Mg^+ was produced by compensating Mg^0 with boron acceptors. The dashed curve is for $\vec{E} \parallel \vec{F}$ and the solid curve is for $\vec{E} \perp \vec{F}$. The arrows indicate the positions of the excitation lines for $\vec{F} = 0$.

patterns. They also imply that the same value of Ξ_u holds for the two cases.

Figs. 18 and 19 show the results for $\vec{F} \parallel [110]$ with $\vec{q} \parallel [001]$ and $\vec{q} \parallel [1\bar{1}0]$, respectively. Both the splittings of the excitation lines and the polarization features agree with the selection rules given in Fig. 6 and Eqs. (3c) and (3d). This is consistent with all the observed transitions originating from a $1s(A_1)$ ground state and with a T_d-symmetry site for Mg^+. The resolution in the measurements was insufficient to separate $2p^a_\pm(+)$ from $2p^b_\pm(+)$ and $2p^a_\pm(-)$ from $2p^b_\pm(-)$.

V. CONCLUDING DISCUSSION

In the present investigation evidence has been accumulated to support the conclusion that magnesium enters the silicon lattice interstitially and as a consequence behaves as a heliumlike double donor. Baxter and Ascarelli[41] have recently carried out an EPR study of magnesium-doped silicon. As is to be expected they have observed EPR only in samples containing Mg^+ donors; using the isotope Mg^{25} they have recorded the hyperfine structure characteristic of it. The excitation spectra and their piezospectroscopic effects as well as EPR studies indicate a T_d site symmetry for the Mg^0 and Mg^+ donors. Thus, the present investigations on magnesium favor the tetrahedral rather than the hexagonal interstitial site. This is also the case for lithium donors in silicon,[12,13] the other interstitial impurity which has been extensively studied.

Another feature which emerges from these studies is how well the effective-mass theory predicts the p states even for donors with ionization energies very much larger than the calculated[26] value of 31.27 meV, e.g., 107.50 meV for Mg^0 and 187.2 meV for one of the neutral sulfur donors.[8] The positions of the $1s(E)$ and $1s(T_2)$ have yet to be experimentally established for both Mg^0 and Mg^+ donors. As discussed in Secs. III A, and IV A these should be close to the effective-mass position for the $1s$ state. Also they should be deeper for a heliumlike donor in comparison to a hydrogenic donor. In this connection the electronic Raman effect[42] should be of particular value. Attention should also be drawn to the fact that whereas for lithium donors in silicon, the $1s(A_1)$ state lies *above* the $1s(E)$ and $1s(T_2)$ states, the opposite is the case for magnesium donors, though both are interstitial impurities.

The value of Ξ_u determined from the piezospectroscopic effect of Mg^0 donors, 8.7 ± 0.2 eV, is in good agreement with that determined for the conduction-band minimum of silicon by a number of different techniques.[43] Krag and his co-workers[8,30] quote a value of 7.9 ± 0.2 eV from the piezospectroscopic effect of sulfur donors and 7.9 eV for phosphorus donors in silicon. It is not clear at the present what the origin is of the difference between our value and those of Krag and co-workers. The values determined from EPR measurements on lithium donors[13] and group-V donors[35] are ~11 eV; the serious discrepancy between the EPR value and the other values has still to be resolved.

ACKNOWLEDGMENTS

The authors wish to thank Professor P. Fisher, Professor J. W. MacKay, Professor S. Rodriguez, Professor G. Ascarelli, and J. E. Baxter for many stimulating discussions. Thanks are due Professor H. J. Yearian and Miss Louise Roth for orienting crystals, to Professor A. N. Gerritsen for supplying the pure magnesium, and to V. J. Tekippe and H. R. Chandrasekhar for help in the quantitative stress measurements.

*Work supported by the NSF and the Advanced Research Projects Agency.

[1]W. Kohn, in *Solid State Physics*, Vol. 5, edited by F. Seitz and D. Turnbull (Academic, New York, 1957), p. 257.

[2]G. W. Ludwig and H. H. Woodbury, in Ref. 1, Vol. 13, p. 223.

[3]P. Fisher and A. K. Ramdas, in *Physics of the Solid State*, edited by S. Balakrishna, M. Krishnamurthi, and B. Ramachandra Rao (Academic, New York, 1969), p. 149.

[4]P. Fisher, R. L. Jones, A. Onton, and A. K. Ramdas, J. Phys. Soc. Japan Suppl. 21, 224 (1966); W. J. Moore, Solid State Commun. 3, 385 (1965).

[5]F. Barra and P. Fisher, Phys. Letters 27A, 711 (1968).

[6]R. A. Chapman and W. G. Hutchinson, Phys. Rev. 157, 615 (1967).

[7]Beryllium in germanium is discussed in the following: H. Shenker, E. M. Swiggard, and W. J. Moore, Trans. AIME 239, 347 (1967); W. J. Moore and R. Kaplan, Bull.

Am. Phys. Soc. 11, 206 (1966); N. D. Tyapkina, M. M. Krivopolenova, and V. S. Vavilov, Fiz. Tverd. Tela 6, 2192 (1964) [Sov. Phys. Solid State 6, 1732 (1965)]. See J. B. Robertson and R. K. Franks, Solid State Commun. 6, 825 (1968) for beryllium in Si.

[8]W. E. Krag, W. H. Kleiner, H. J. Zeiger, and S. Fischler, J. Phys. Soc. Japan Suppl. 21, 230 (1966).

[9]G. W. Ludwig, Phys. Rev. 137, A1520 (1965).

[10]D. L. Camphausen, H. M. James, and R. J. Sladek, Phys. Rev. B 2, 1899 (1970).

[11]P. Fisher and H. Y. Fan, Phys. Rev. Letters 5, 195 (1960); R. L. Jones, P. Fisher, and S. Balasubramanian (unpublished).

[12]R. L. Aggarwal, P. Fisher, V. Mourzine, and A. K. Ramdas, Phys. Rev. 138, A882 (1965).

[13]G. D. Watkins and F. S. Ham, Phys. Rev. B 1, 4071 (1970).

[14]H. H. Woodbury and G. W. Ludwig, Phys. Rev. 117, 102 (1960); G. W. Ludwig and H. H. Woodbury, Phys. Rev. Letters 5, 98 (1960).

[15]G. D. Watkins, *Radiation Damage in Semiconductors, Paris-Royaumont*, 1964 (Dunod, Paris, 1965), p. 97.

[16]R. K. Franks and J. B. Robertson, Solid State Commun. 5, 479 (1967).

[17]L. T. Ho and A. K. Ramdas, Phys. Letters 32A, 23 (1970). This paper contains a preliminary account of the results presented here.

[18]Magnesium of 99.9948% purity, Dow Chemical Company, Midland, Michigan.

[19]R. D. Hancock and S. Edelman, Rev. Sci. Instr. 27, 1082 (1956).

[20]P. Fisher, W. H. Haak, E. J. Johnson, and A. K. Ramdas, in *Proceedings of the Eighth Symposium on the Art of Glassblowing* (The American Scientific Glassblowers Society, Wilmington, Delaware, 1963), p. 136.

[21]A. C. Rose-Innes, Proc. Phys. Soc. (London) 72, 514 (1958). Details of the jigs used in the differential compression technique are given in R. L. Jones, Ph.D. thesis (Purdue University, 1968) (unpublished).

[22]V. J. Tekippe, P. Fisher and A. K. Ramdas (unpublished).

[23]Charles M. Reeder & Co., Inc., Detroit, Michigan.

[24]R. L. Aggarwal and A. K. Ramdas (unpublished).

[25]C. E. Moore, *Atomic Energy Levels*, Natl. Bur. Std. (U.S.) Circ. No. 467 (U.S. GPO, Washington, D. C., 1949), p. 5; see also H. G. Kuhn, *Atomic Spectra* (Academic, New York, 1963), p. 132; and H. A. Bethe and E. E. Salpeter, *Quantum Mechanics of One- and Two-Electron Atoms* (Springer-Verlag, Berlin, 1957), p. 127.

[26]R. A. Faulkner, Phys. Rev. 184, 713 (1969).

[27]The donor states are labeled according to the envelope wave function (1*s*, 2*s*, ..., etc.) and the irreducible representations of the site symmetry of the donor. Evidence presented in this paper suggests that the latter is T_d for both Mg^0 and Mg^+. Note that the notation for the irreducible representations follows Ref. 1, however, with labels T_1 and T_2 interchanged to conform to the usage current in the literature. See, for example, H. Eyring, J. Walter, and G. E. Kimball, *Quantum Chemistry* (Wiley, New York, 1944), p. 388, Table 37; E. B. Wilson, Jr., J. C. Decius, and P. C. Cross, *Molecular Vibrations* (McGraw-Hill, New York, 1955), p. 330, Table X-10, where $T_1 \equiv F_1$ and $T_2 \equiv F_2$. Readers should note that much of the earlier literature on donors use T_1 and T_2 as in Ref. 1.

[28]W. H. Kleiner and W. E. Krag, Phys. Rev. Letters 25, 1490 (1970).

[29]R. L. Aggarwal and A. K. Ramdas, Phys. Rev. 140, A1246 (1965).

[30]W. E. Krag, W. H. Kleiner, and H. J. Zeiger, *Proceedings of the Tenth International Conference on the Physics of Semiconductors, Cambridge, Mass.*, 1970, edited by S. P. Keller, J. C. Hensel, and F. Stern (U. S. AEC Division of Technical Information, Washington, D. C., 1970), p. 271.

[31]B. T. Ahlburn and A. K. Ramdas, Phys. Rev. 167, 717 (1968).

[32]T. E. Gilmer, Jr., R. K. Franks and R. J. Bell, J. Phys. Chem. Solids 26, 1195 (1965).

[33]R. L. Aggarwal and A. K. Ramdas, Phys. Rev. 137, A602 (1965).

[34]C. Herring, Bell System Tech. J. 34, 237 (1955); see also C. Herring and E. Vogt, Phys. Rev. 101, 944 (1956).

[35]D. K. Wilson and G. Feher, Phys. Rev. 124, 1068 (1961).

[36]A. A. Kaplyanskii, Opt. i Spektroskopiya 16, 602 (1964); 10, 165 (1961) [Opt. Spectry. (USSR) 16, 329 (1964); 10, 83 (1961)].

[37]This feature was experimentally observed in the course of a recent study of the excitation spectra of P and As donors in silicon by V. J. Tekippe, H. R. Chandrasekhar, P. Fisher, and A. K. Ramdas (unpublished). The details of the data processing used in Figs. 11 and 12 will be given in this paper.

[38]This was pointed out to us by Professor P. Fisher. Our thanks are due him and Professor S. Rodriguez for several discussions on this aspect.

[39]Our thanks are due to Professor J. W. MacKay for this suggestion.

[40]See H. H. Woodbury and G. W. Ludwig, Phys. Rev. Letters 5, 96 (1960), where a conversion of an interstitial impurity into a substitutional one by trapping a vacancy has been considered. Ludwig has also discussed it in Ref. 9 in the context of the substitutional vs interstitial nature of S^+ donors in silicon.

[41]J. E. Baxter and G. Ascarelli (unpublished).

[42]G. B. Wright and A. Mooradian, Phys. Rev. Letters 18, 608 (1967).

[43]L. D. Laude, F. H. Pollak, and M. Cardona, Phys. Rev. B 3, 2623 (1971); I. Balslev, Phys. Rev. 143, 636 (1966); see also the concluding sections in Refs. 13 and 29.